9

Ferroelectric Copolymer-Based Plastic Memory Transistos

Sung-Min Yoon[1] et al.*
[1]*Dept. Advanced Materials Engineering for Information & Electronics, Kyung Hee University*
Korea

1. Introduction

Flexible electronic devices and systems fabricated on bendable, rollable, and stretchable plastic substrate define important application fields of novel paradigm for next-generation ”consumer electronics”. In these fields, such features as good design, ultra-low cost, and unique functionality would be primarily demanded, which is totally different from the case of conventional Si-based electronics. Recently, many types of interesting approaches have been actively researched and developed. Flexible displays (Gelinck & Leeuw, 2004; Park J. S. et al., 2009), radio-frequency flexible identification tags (Forrest, 2004; Jung M. et al., 2010), flexible and stretchable sensor arrays (Lin K. & Jain, 2009; Someya et al., 2005), flexible electronic circuit systems (Graz & Lacour, 2009; Zschieschang et al, 2010), stretchable lightings (Sekitani et al., 2009a), printable devices (Ishida et al., 2010), and sheet-type communication and power-transmission system (Sekitani et al., 2009b) are the feasible examples. In order to develop the practical systems using these devices, an embeddable nonvolatile memory is strongly required as one of the core devices. The employment of suitable memory device into the systems can effectively reduce their power consumption (Chu et al., 2010; Ueda et al., 2010) as well as enhance their functions by storing the information. Therefore, if the nonvolatile memory devices having features of mechanical flexibility, lower power operation, higher device reliability, and simpler fabrication process at lower temperature would be successfully realized, it would make great impacts on the related fields.

So far, various methodologies using different operating origins and material combinations have been tried to realize the nonvolatile memory functions on the flexible plastic substrates. They can be roughly classified into several types according to the active materials and device structures. Reversible resistance change in organic layer has been exploited for the plastic memory applications, which is operated by reduction-oxidation reaction of the organic layer (Novak et al., 2010), charge-trapping/detrapping within the organic composite (Cho B. et al., 2010) or conductive filament formation between the top and bottom electrodes sandwiching

*Shinhyuk Yang[2], Soon-Won Jung[3], Sang-Hee Ko Park[4], Chun-Won Byun[5], Min-Ki Ryu[6], Himchan Oh[7], Chi-Sun Hwang[8], Kyoung-Ik Cho[9] and Byoung-Gon Yu[10]
[2,3,4,5,6,7,8,9,10]*Convergence Components & Material Research Lab., Electronics and Telecommuncation Research Institute (ETRI), Korea*

the organic films (Ma et al., 2004). The bending characteristics of the resistive-type nonvolatile polymer memory device fabricated on the poly(ethylene terephthalate) were well demonstrated (Ji Y. et al., 2010). In place of organic layers, binary oxide thin-films which can be deposited at low temperature were also employed for the resistance change operation (Lee S. et al., 2009; Seo J. W. et al., 2009). The feasibility for the three-dimensional stacked memory concept was also introduced by implementing one-diode (CuO/InZnO)-one-resistor (NiO) storage node with InGaZnO (IGZO) thin-film transistors (Lee M. J. et al., 2009). Charge-injection has also been utilized for the nonvolatile memory operation, for which specified device structures such as organic bilayers (Ma et al., 2002) or nanoparticle-embedded organic layers (Leong W. L. et al., 2009) have been proposed. Organic thin-film transistor having a floating-gate for charge storing is one of the most typical memory transistors fabricated on the plastic substrates (Baeg K. J., 2010; Wang W. et al., 2009). On the other hand, the ferroelectric-based field effect transistor (FeFET) have features that remnant polarization of ferroelectric gate insulator can be employed for the nonvolatile memory actions (Kang S. J. et al., 2009a; Lim S. H. et al., 2004). Although each device configuration has pros and cons, the practical memory array embeddable into the flexible electronic systems have not been yet commercialized.

Tracing the nonvolatile memory technologies in Si-based electronics back to 1990s, the FeFET was one of the most promising devices replacing the conventional flash memory facing physical scaling limitations at those times. However, the crosstalk for random accessibility and short data retention time of the FeFET were concluded to be fatal drawbacks for the mass-production, although it successfully claimed the ultimate scalability and nondestructive readout characteristics. Unlike these situations in the Si-based electronics demanding an ultra-high specifications and an aggressive device scaling, the requirements for the nonvolatile memory devices integrated into the large-area electronics including the flexible systems are considerably different. In these fields, low-cost and stable operation would be more important factors than the high performances. From this viewpoint, the ferroelectric field-effect thin-film transistor employing a polymeric ferroelectric material, instead of oxide ferroelectrics, can be a very promising candidate because it can be operated in a very reproducible way with a definitely designable operation principle and be fabricated by a very simple process. In this chapter, we propose the organic/inorganic hybrid-type plastic memory transistor exploiting the ferroelectric field effect with the gate stack structures of ferroelectric copolymer gate insulator and oxide semiconducting active channel. Our device concept and features of ferroelectric copolymer-based memory transistor will be proposed in Section 2. The device characteristics and nonvolatile memory behaviors of the proposed plastic memory transistors are demonstrated and the remaining technical issues to solve for future practical applications are picked up. This approach will provide a special meaning to expand the ferroelectric nature to the next-generation large-area electronics.

2. Flexible ferroelectric memory

As mentioned above, the single-transistor-cell-type memory transistors composed of a ferroelectric gate insulator (GI) have been extensively investigated for the conventional Si electronics so far, in which various oxide ferroelectric materials such as $Pb(Zr,Ti)O_3$ (Shih W. C. et al., 2007; Tokumitsu et al., 1997), $SrBi_2Ta_2O_9$ (Horiuchi et al., 2010; Tokumitsu et al., 1999; Yoon S. M. et al., 1999), $(Bi,La)_4Ti_3O_{12}$ (Aizawa K. et al., 2004; Lee N. Y. et al., 2003),

$PbGeO_3$ (Li T. et al., 2003), $YMnO_3$ (Ito D. et al., 2003), $LiNbO_3$ (Kim K. H., 1998), and $BiFeO_3$ (Lin C. et al., 2009) have been chosen as the ferroelectric GI. However, in realizing the plastic nonvolatile memory array, the use of oxide ferroelectric GI is absolutely unfavorable owing to the high crystallization temperature which is typically higher than 650 °C. The overall process temperature should be suppressed below 200 °C. Although some encouraging reports on the novel transfer technique (Roh J. et al., 2010) and ultra-low temperature process (Li J. et al., 2010) for the oxide ferroelectric thin films have recently been published, to secure the high-quality oxide ferroelectric GI for the memory transistor with low temperature process is still very challenging. From this background, the employment of polymeric ferroelectric thin film can offer an attractive solution to this problem because its crystallization temperature is much lower than those of the oxide ferroelectrics. Poly(vinylidene fluoride-trifluoroethylene) [P(VDF-TrFE)] is the most typical ferroelectric copolymer material (Furukawa T., 1989; Nalwa H. S., 1995). It shows superior properties of a relatively large remnant polarization, a short switching time, and a good thermal stability when it is compared with other organic ferroelectric materials such as odd-nylon, cynopolymer derivatives, polyurea, ferroelectric liquid crystal polymers (Nalwa H. S., 1995). The melting temperature, Curie temperature, and crystallization temperature are changed with the composition of PVDF and TrFE. For the composition of 70/30 mol% for the P(VDF-TrFE), those properties are known as 155 °C, 106 °C, and 129 °C, respectively. The remnant polarization (P_r) and dielectric constant are in the ranges from 8 to 12 $\mu C/cm^2$ and from 12 to 25 , respectively, depending on the composition (Nalwa H. S., 1995). P(VDF-TrFE) thin film can be simply formed by a solution-based spin-coating method and be crystallized at a lower temperature around 140 °C, which is one of the beneficial merits in realizing the memory device on the plastic substrate.

So far, most works on the fabrication and characterization for the nonvolatile memory transistors using the P(VDF-TrFE) have been mainly investigated for realizing the all-organic memory transistors with organic semiconducting channel layers. Various organic active layers such as the evaporated pentacene (Kang S. J. et al., 2008; Nguyen C. A. et al., 2008; Schroeder R. et al., 2004), soluble pentacene (Kang S. J. et al., 2009a;b), and solution-processed polymeric semiconductors (Naber R. C. G. et al., 2005a;b) were chosen and the memory thin-film transistors were demonstrated. Actually, it is the case that the employment of organic channel can be very suitable for low-cost disposable applications with a lower specification. However, the weaknesses of a low field-effect mobility, a unsatisfactory ambient stability, and a difficult device integration with the organic-based transistors seriously restrict the real application of this kind of memory TFT within narrow limits. A powerful alternative for enhancing and stabilizing the device performance is to utilize the oxide semiconductor such as ZnO and IGZO, which is one of the most important features of our proposed plastic memory transistor. The oxide semiconductor-based TFTs present such beneficial features as high field-effect mobility, excellent uniformity, and robust device stability (Hoshino K. et al., 2009; Jeong J. K. et al., 2008; Nomura et al., 2004). As results, the oxide TFTs have attracted huge interest as one of the most promising backplane device technologies for the next-generation liquid-crystal display (LCD) (Osada T. et al., 2010) or organic light-emitting diode display (OLED) (Ohara H. et al., 2010; Park J. S. et al., 2009) with a large size and a high resolution. A transparency of the oxide semiconductor to the visible light can be another benefit of expanding the applications to the transparent electronic devices (Park S. H. et al., 2009). These features can be similarly applied for the ferroelectric-based plastic memory transistors. Because the oxide channels are patterned into only small gate areas on the substrate, a relatively brittle nature of oxide

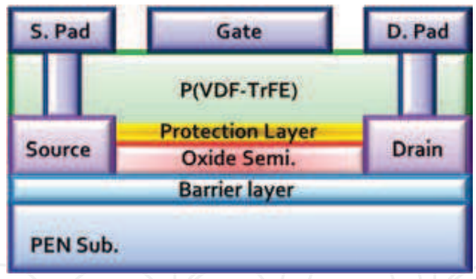

Fig. 1. Typical example of a schematic cross-section diagram for the proposed plastic memory TFT.

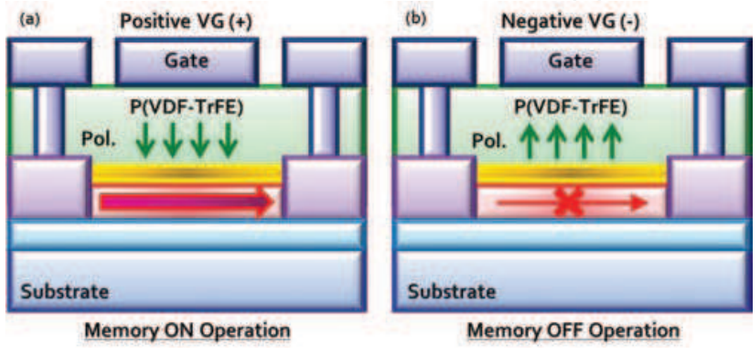

Fig. 2. Schematic views on the operating origin for the nonvolatile memory behaviors of the ferroelectric field-effect-driven memory TFT. When the oxide semiconductor is considered to be n-type, positive and negative programming voltage are initially applied to the gate terminal for (a) *on* and (b) *off* operations, respectively.

thin-film will be no longer a fatal problem for the flexible electronic devices. The use of oxide channel for the plastic memory TFT is also preferable in the viewpoint of integrating the full-scale memory array with memory cells and peripheral driving circuit. Because the oxide TFTs are very suitable devices composing the circuit components, we can design the process using common oxide channels for both the memory and driving TFTs. On the basis of the considerations discussed above, the combination of an organic ferroelectric gate insulator and an oxide semiconducting channel will be the best choice for the high performance nonvolatile memory transistors embeddable into the various electronic systems implemented on the large-area flexible plastic substrate.

Figure 1 shows a typical schematic cross-sectional view of our proposed plastic memory TFT, which was designed to be a top-gate bottom-contact configuration. Because the P(VDF-TrFE) is vulnerable to the plasma-induced deposition process for the oxide channel layer, the bottom-gate configuration is very difficult to be fabricated with an excellent interface between the P(VDF-TrFE) and oxide semiconductor. Furthermore, in order to enhance the device performances, the post-annealing process is sometimes performed at a temperature higher than 200 °C after the deposition of oxide channel. However, the available thermal budget after the formation of P(VDF-TrFE) is restricted to below 150 °C for the bottom gate structure owing to the low melting temperature of the P(VDF-TrFE). The interface controlling layer in the top-gate structure, as shown in the figure, is very desirable to be introduced between the P(VDF-TrFE) and oxide channel layer. In this work, a very thin Al_2O_3 layer deposited by

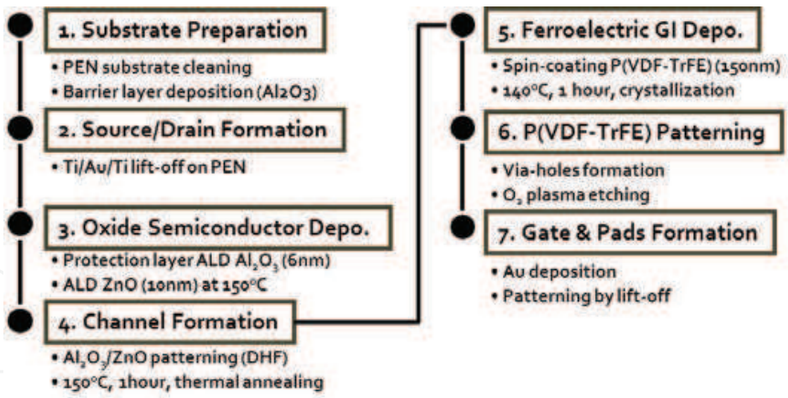

Fig. 3. Flowchart of fabrication procedures for the proposed plastic memory TFT, in which the process steps were designed to use four photomasks. All processes were performed below 150 °C.

atomic-layer deposition (ALD) method was prepared for the device fabrication. This interface controlling layer is very effective for protecting the channel surface during the coating and etching processes of the P(VDF-TrFE) GI layer. Chemical solvents of the P(VDF-TrFE) solution and/or oxygen plasma environment employed for the P(VDF-TrFE) patterning process might degrade the electrical natures of the oxide channel layers. The operating origin for the nonvolatile memory behaviors of the proposed memory TFT can be explained by simple schematics shown in Fig. 2. When the positive gate voltage is applied, the ferroelectric polarization of the P(VDF-TrFE) aligns downward and hence the large drain current flow in the n-type oxide channel layer between the source and drain terminals. Because the aligned polarization remained even after the removal of the gate voltage, the programmed drain current can be detected when the drain is biased. This is the memory *on* state. On the other hand, after the negative gate voltage is applied, the polarization aligns upward, and hence the device doesn't flow the current through the channel. This is the memory *off* state. The programmed data can be nondestructively readout in the shape of drain current, because the read-out signals are so chosen as not to reverse the direction of pre-aligned ferroelectric polarization. In order to guarantee the good memory operations of the proposed memory TFT, it is very important to carefully design and optimize some parameters of thicknesses in the interface controlling and oxide channel layers. The detailed strategies can be referred in our previous investigation (Yoon S. M. et al., 2009a). We previously demonstrated the feasibility of our proposed memory TFTs fabricated on the glass substrate. The excellent device characteristics of the memory TFT using P(VDF-TrFE) GI and IGZO active channel was successfully confirmed, in which a thermal budget for overall process was 250 °C (Yoon S. M. et al., 2010a). The fully-transparent memory TFT using Al-Zn-Sn-O active channel was fabricated to have the transmittance of approximately 90% at a wavelength of 550 nm (Yoon S. M. et al., 2010b). Write and read-out operations of the two-transistor-type memory cell composed of one-memory and one-access oxide TFTs, which was integrated onto the same substrate, were also demonstrated (Yoon S. M. et al., 2010c). In this work, we will focus on the fabrication and characterization of the flexible nonvolatile memory TFT prepared on the plastic substrate.

3. Experimetal details

Poly(ethylene naphthalate) (PEN, Teijin DuPont) was selected as a substrate owing to its low coefficient of thermal expansion, strong chemical resistance, and low-cost for the device fabrication. Firstly, barrier against the out-gassing and surface planarization layer of ALD-grown Al_2O_3 was prepared onto the bare PEN substrate. Ti/Au/Ti film was deposited by electron-beam (e-beam) evaporation and patterned into the source/drain electrodes on the 200-μm-thick PEN by lift-off process. Top and bottom layers of Ti worked as good ohmic contact with oxide channel layer and good adhesion with the substrate, respectively. 10-nm-thick ZnO film was chosen as an oxide semiconducting channel for the plastic memory TFT, which was deposited by plasma-enhanced ALD method at 150 °C using diethylzinc and O_2 plasma as the Zn and oxygen sources, respectively. Then, 6-nm-thick Al_2O_3 interface controlling layer was successively deposited by ALD method at 150 °C using trimethylaluminium and water vapor as the Al and oxygen sources, respectively. After the Al_2O_3 and ZnO were patterned into the channel areas using dilute hydrofluoric acid solution, thermal treatment was performed at 150 °C to enhance the ZnO channel properties. P(VDF-TrFE) layer was formed by spin-coating method using a 2.5 wt% dilute solution of P(VDF-TrFE) (70/30 mol%) in methyl-ethyl-ketone. A solution was spun on the substrate at a spin rate of 2000 rpm and then dried at 70 °C for 5 min on a hot plate. The prepared film was crystallized at 140 °C for 1 h in an air ambient. The film thickness of P(VDF-TrFE) was measured to be approximately 150 nm. Via-holes were formed by O_2 plasma etching of the given areas of P(VDF-TrFE) layer using a dry etching system, in which the lithography processes including the developing and stripping of photoresists coated on the P(VDF-TrFE) layer were so carefully designed as not to make undesirable chemical damage to the P(VDF-TrFE) (Yoon S. M. et al., 2009b). Finally, Au film was deposited by e-beam evaporation and patterned as gate electrode and pads via lift-off process. The process flow and the detailed conditions were summarized in Fig. 3. Figures 4(a) and (b) show a photograph of the process-terminated PEN substrate and a typical photo-image of the substrate under a bending situation, respectively. The size of the test-vehicle processed on the PEN substrate was 2×2 cm^2. The microscopic top view of the memory TFT fabricated on the PEN substrate was shown in Fig. 4(c). All the electrical characteristics including programming and retention behaviors of the fabricated plastic memory TFT were evaluated in a dark box at room temperature using a semiconductor parameter analyzer (Agilent B1500A). The variations in their characteristics under the bending situation with a given curvature radius (R) were measured by setting the configuration, as shown in Fig. 4(d).

4. Device evaluations

4.1 Bending characteristics of ferroelectric P(VDF-TrFE) capacitors

In advance, the basic ferroelectric behaviors were investigated for the P(VDF-TrFE) capacitors which were fabricated with the TFTs on the same substrate. Figure 5(a) and (b) show a schematic cross-sectional diagram and a top-view of optical microscope for the Au/P(VDF-TrFE)/Au capacitors. Patterned P(VDF-TrFE) film was accurately defined between the top and bottom electrodes with the capacitor size of 25×25 μm^2. The polarization-electric field (P-E) characteristics of the ferroelectric capacitor were measured as shown in Fig. 5(c), in which the E was modulated from 0.45 to 1.80 MV/cm. Typical values

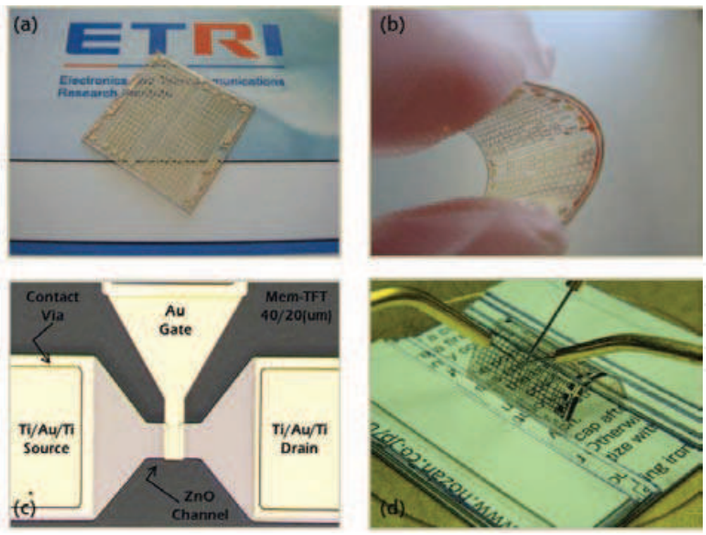

Fig. 4. (a) A Photograph of the PEN substrate on which the test devices were fabricated. (b) A typical photo image of the PEN substrate under a bending situation. The substrate size is 2×2 cm^2. (c) Microscopic top view of the fabricated memory TFT with the structure of Au/P(VDF-TrFE)/Al_2O_3/ZnO/Ti/Au/Ti/Al_2O_3/PEN. The channel width and length are 40 and 20 μm, respectively. (d) A photo image of electrical evaluation for the fabricated device when the PEN substrate was bent with R of 0.65 cm.

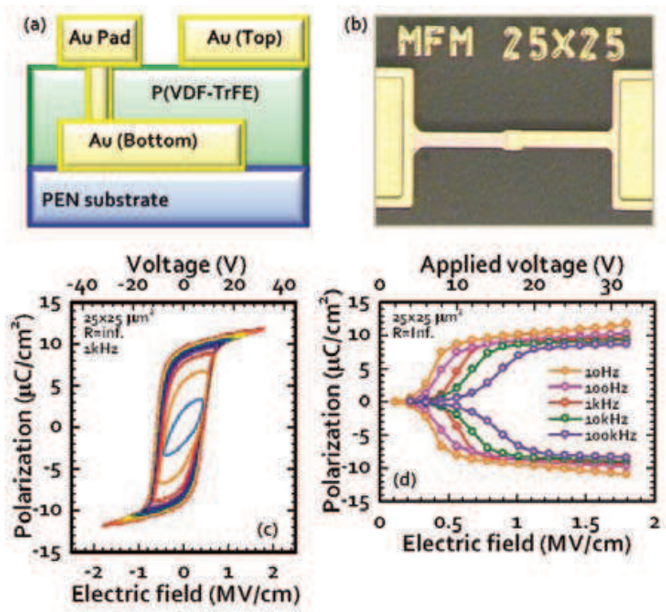

Fig. 5. (a) A Schematic cross-sectional diagram and (b) a microscopic image of the evaluated P(VDF-TrFE) capacitors fabricated on the PEN substrate. The patterned capacitor size was 25×25 μm^2. (c) A typical P-E characteristics of the P(VDF-TrFE) capacitors fabricated on the PEN substrate at the frequency of 1 kHz. (d) Polarization saturation behavior with the increase in the E applied across the capacitor at various signal frequencies from 10 Hz to 100 kHz.

of the remnant polarization (P_r) and coercive field (E_c) were obtained to be approximately 9.1 μC/cm^2 and 522 kV/cm, respectively, at the measuring signal frequency of 1 kHz. The polarization saturation behaviors with the increase of the E applied across the ferroelectric film were also examined at various signal frequencies from 10 Hz to 100 kHz, as shown in Fig. 5(d). The E required to obtain the full saturation in the ferroelectric polarization was observed to decrease with the decrease in signal frequency, which is related to the fact that the memory operations of the proposed plastic memory TFT may be influenced by the duration of programming voltage signals as well as the signal amplitudes (Furukawa T. et al., 2006; 2009; Yoon S. M. et al., 2010d). It can be said that these obtained characteristics were almost similar to those for the P(VDF-TrFE) capacitors fabricated on the Si or glass substrate, even they were prepared on the flexible PEN substrate.

It is very important to investigate the variations in electrical properties of the fabricated capacitors when the substrate was bent with a given curvature radius (R). In these measurements, the R was set to be two values of 0.97 and 0.65 cm, as shown in Figs. 6(a) and (b), respectively, which visually show the bending situations of the substrate. Figures 6(c) and (d) show the P-E ferroelectric hysteresis curves of the same device examined in Fig. 5 when the R's were 0.97 and 0.65 cm, respectively. There was no problem in obtaining the ferroelectric polarization for the P(VDF-TrFE) capacitors even under the bending situations. The detailed variations with the changes in R can be confirmed in Fig. 7(a), in which P-E curves obtained at the same field for the bending situations with different R's were compared. The P_r was varied to approximately 9.6 μC/cm^2 when the R decreased to 0.65cm, which correspond to the increase by 5% compared with the case when R was infinite (∞). However, this small increase in P_r can be explained by the increase in leakage current component for the examined device owing to the repeated evaluations under a high electric field. As a result, it can be suggested that the capacitor did not experience a significantly remarkable variation in the ferroelectric properties. On the other hand, the E_c was measured to be approximately 528 and 588 kV/cm when the R was set to be 0.97 and 0.65 cm, respectively. Although it was observed that there was an approximately 13% increase in E_c when the substrate was bent with R of 0.65 cm, it is likely that this does not originated from the mechanical strain induced by the substrate bending. The detailed effects of the bending R on the polarization saturation behaviors were examined as shown in Figs. 7(c) and (d) at two signal frequencies of 10 Hz and 10 kHz, respectively. It is very useful to introduce a parameter of E_{hp} in order to quantitatively compare the obtained characteristics for the different bending situations. The E_{hp} was defined as the electric field required for securing the half point of full saturation of ferroelectric polarization ($0.5P_r$) at a given signal frequency. For the signal frequency of 10 Hz [Fig. 7(c)], the E_{hp}'s for the various R's of ∞, 0.97, and 0.65 cm were estimated to be approximately 0.38, 0.41, and 0.44 MV/cm, respectively. On the other hand, at the signal frequency of 10 kHz [Fig. 7(d)], the E_{hp}'s were approximately 0.67, 0.72, and 0.81 MV/cm for the same situations. These observations might indicate that the polarization switching at initial phase for the lower electric field was impeded when the P(VDF-TrFE) film was bent, and that the extent of impediment was larger for the cases of larger R and higher signal frequency. However, these kinds of evaluation are sometimes very tricky and controversial. It was also observed that the E_{hp} showed larger values when the substrate was restored to the initial flat status (R=∞) compared with those for the R of 0.65 cm, as shown in Figs. 7(c) and (d). Consequently, it can be concluded that the larger impediment in polarization switching event, which was mainly observed for the larger R, was dominantly affected by the ferroelectric fatigue, even

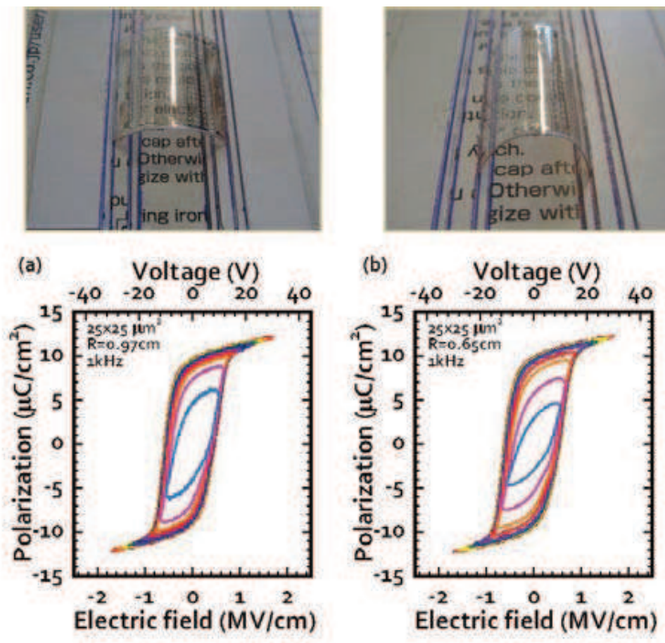

Fig. 6. *P-E* characteristics of the Au/P(VDF-TrFE)/Au capacitors when the substrate was bent with different R's of (a) 0.97 and (b) 0.65 cm. The bending situations of each case are shown in photos. The measurement frequency was set to be 1 kHz.

though some parts of degradation caused by the mechanical strain at the bending situation cannot be completely ruled out. It gives more detailed insights to investigate the bending characteristics of the device with different capacitor size, as shown in Fig. 7(b), because the mechanical strain is differently induced for the capacitors with different size even for the same R. According to the obtained characteristics for the P(VDF-TrFE) capacitors with the size of 200×200 μm^2, there was not any marked variation in the behaviors except for the small increase in E_c with the decrease of R. It suggests that the polarization saturation behaviors behaved in a very similar way to those discussed above for the 25×25-μm^2-sized capacitor even for the larger capacitor size. We can found from these discussions that the mechanical strain applied to the P(VDF-TrFE) capacitors under the bending situations did not make any critical influence on the ferroelectric properties, which is in a good agreement with the previous reports (Matsumoto A. et al., 2007; Nguyen C. A. et al., 2008). However, the data reproducibility and further investigations should be also performed with smaller R to accurately verify the bending effects on the device as future works.

4.2 Memory behaviors of flexible memory TFT

Based on the basic ferroelectric properties of the P(VDF-TrFE) capacitors fabricated on the PEN substrate, the device characteristics of the fabricated memory TFT were extensively investigated. Figure 8(a) shows the drain current-gate voltage (I_D-V_G) transfer characteristics of the plastic memory TFT at the various sweep range in V_G, which were measured with a double sweep mode of forward and reverse directions at V_D of 5.0 V. The gate width (W) and length (L) of the measured device were 40 and 20 μm, respectively. As can be seen in the figure, we could obtain sufficiently good device performances, in which the 8-orders-of

magnitude on/off ratio and the subthreshold swing (SS) of 650 mV/dec were successfully obtained. Counterclockwise hystereses of the transfer curves which originated from the ferroelectric field effect were clearly observed. A 3.4 V-memory window was obtained at the V_G sweep range from -10 to 8 V. Gate leakage currents could be suppressed to be lower than 10^{-11} A, even though the device was fabricated on the plastic substrate using low-temperature processes below 150 °C. It was confirmed that the transfer characteristics did not change between the first and the second sweep in V_G, as shown in Fig. 8(b). This is also an important point considering the fact that the transfer curves of this kind of memory TFT are markedly fluctuated if the fabrication processes are not optimized for the device. Although only twice repetitive measurements of transfer curves cannot guarantee the endurance in device performance, the undesirable variations in device characteristics during the repetitive operations could be easily examined even by performing only two successive sweeps. Therefore, it can be concluded that the proposed plastic memory TFT was well fabricated on the PEN substrate without any critical damages caused by fabrication processes. The bending characteristics were also investigated for the same device, in which two kinds of measurements were performed. The first one is to examine the changes in device behaviors at the situations of substrate bending with a given R, which can be called as "bending durability". The second one is to evaluate the degradation in device performance after the given numbers of repetitive bending operation, which can be called as "bending fatigue endurance". Figure 9(a) shows the bending durability by measuring the transfer characteristics when the substrate was bent with the R of 0.97 cm. As can be seen in the figure, the plastic memory TFT did not experience so marked variations in its device behaviors. The change in memory window at the bending situation was approximately 0.7 V at most. It was also very encouraging that the bending fatigue endurance test with 20,000 cycles did not make any critical degradation in its characteristics, as shown in Fig. 9(b). In this evaluation, bending fatigue was intentionally loaded by using the specially-designed bending machine shown in Figs. 9(c) and (d), in which the R was set to be 2.35 cm. These results indicate that the proposed plastic memory TFT fabricated on the PEN can be utilized under the bending situations for any flexible devices. Although the R could not be reduced to smaller state owing to the substrate size and machine specification in this work, further investigations would be necessary when the device is repeatedly bent for larger number of bending at smaller R. Actually, we have to check the observation that a very small reduction in the memory window was observed as the increase in the number of bending.

Finally, the programming and retention behaviors of the fabricated plastic memory TFT were evaluated, as shown in Fig. 10. These characteristics are very important for actually employing the nonvolatile memory component embedded into the large-area flexible electronic systems. The programming events for the *on* and *off* states were performed by applying the voltage pulses of 6 and -8 V, respectively. The pulse width was varied to 1 s and 100 ms in order to estimate the relationship between the available memory margin and the programming time. Both memory states were detected by measuring the I_D at a read-out V_G of 0 V. The memory window in transfer curve for the memory TFT, which was obtained to be located with centering around 0 V in V_G [Fig. 8], is a very beneficial property, because the read-out and retention operations for the stored information can be carried out at 0 V. For the case of 1 s-programming, the *on*/*off* ratio was initially obtained to be approximately 6.6×10^5 and it decreased to approximately 130 after a lapse of 15000 s. On the other hand, for the case of 100 ms-programming, the initial *on*/*off* ratio was only 8.0×10^3 and the memory margin

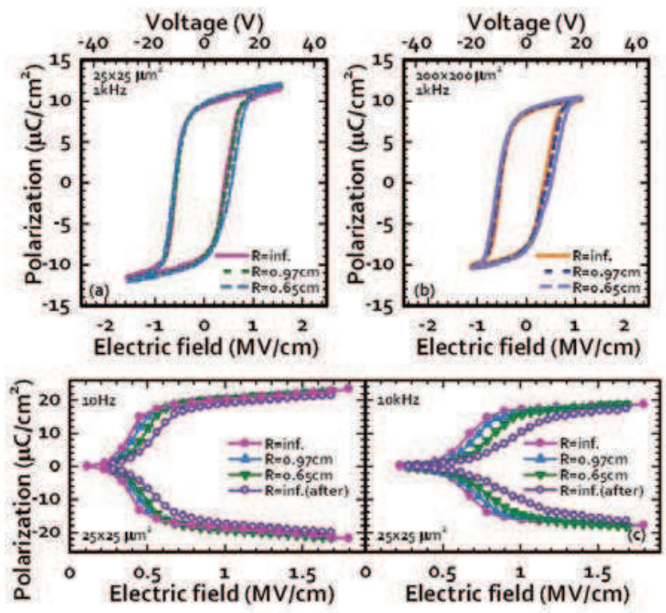

Fig. 7. Comparisons of the *P*-*E* characteristics of the fabricated capacitors with the size of (a) 25×25 μm^2 and (b) 200×200 μm^2 when the R was varied to ∞, 0.97 and 0.65 cm. For the case of 25×25 μm^2-sized capacitor, the polarizarization saturation behaviors were investigated at the signal frequencies of 10 Hz and 10 kHz when the R was varied to ∞, 0.97, 0.65 cm and restored to initial ∞ state.

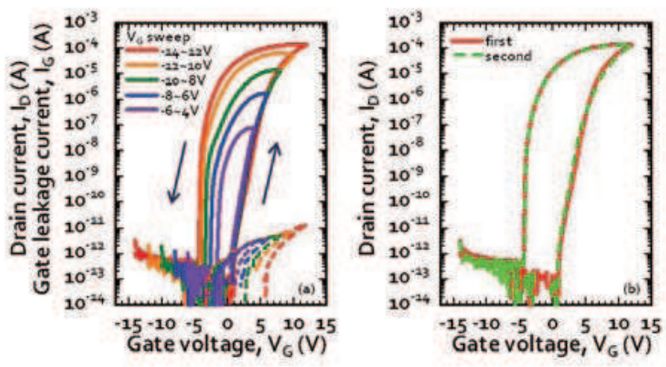

Fig. 8. (a) Sets of I_D-V_G transfer curves and gate leakage currents of the fabricated nonvolatile plastic memory TFT fabricated on the PEN substrate when the V_G sweep ranges were varied. (b) Variations of transfer characteristics of the same device between the first and the second sweeps in V_G. The V_D was set to be 5 V. The channel width and length of the evaluated device was 40 and 20 μm, respectively.

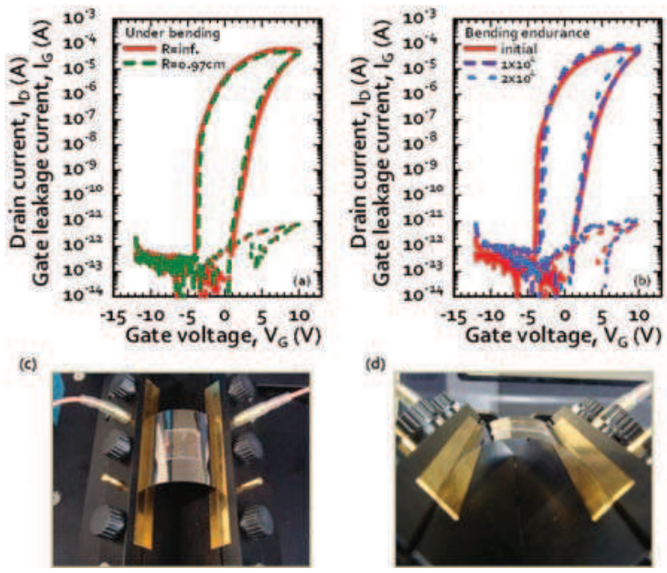

Fig. 9. Variations of transfer charactristics and memory behaviors of the fabricated plastic memory TFT (a) under the substrate bending situation with *R* of 0.97 cm and (b) after the 20,000 cycles of repetitive bending operations with the *R* of 2.35 cm. (b) Typical photo images of the bending fatigue evaluation performed by a specially-designed bending machine.

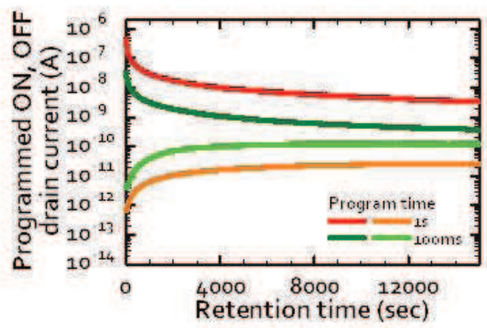

Fig. 10. Data retention behaviors of the fabricated plastic memory TFT as the changes in programmed I_D with a lapse of 15,000 s. The *on* and *off* states were programmed by applying the voltage pulses of 6 and -8 V, respectively. The pulse width was varied to 1 s and 100 ms.

almost disappeared during the retention phase. Although it was sufficiently encouraging to confirm the practical *on*/*off* ratio of higher than 2-orders-of magnitude for the fabricated plastic memory TFT even after a lapse of 4 hours, the programming and retention behaviors should be much more improved for real applications. The remaining issues and feasible appropriate solutions will be discussed in the next section.

5. Remaining issues

In previous sections, the promising methodologies and technical feasibilities were described for utilizing our proposed plastic memory TFTs prepared on the PEN substrate as core

memory devices for the future large-area flexible electronics. However, some technical issues remain to meet the required specifications. The first one is that the memory device reliabilities, especially data retention, were not so satisfying at this stage. The typical retention times of the previously reported memory TFT employing the polymeric ferroelectric GI and oxide channel are still in the range of several hours even when they were fabricated on the glass substrate (Lee K. H. et al., 2009a; Noh S. H. et al., 2007; Park C. H. et al., 2009). Three significant factors that critically affect the retention behaviors are intrinsic depolarization field, gate leakage components, and interface quality. The detailed features and solutions for each factor can be retrieved in our previous article (Yoon S. M. et al., 2011a). Considering the feasible applications utilizing the proposed flexible memory TFT, it is not necessary to guarantee years-of retention time. However, the stability of the stored data during several days will surely expand the application fields of the proposed flexible nonvolatile memory TFT. The second issue is that the obtained programming characteristics were sensitively dependent on the pulse width. Furthermore, the required duration for the stable programming was observed as long as 1 s, which has also been reported in other publications on the polymeric ferroelectric GI-based memory TFTs (Choi C. W. et al., 2008; Lee K. H. et al., 2009b; Uni K. N. N. et al., 2004). These properties have a direct influence on the programming speed of the flexible memory device. The discussions on the programming speed was also intensively discussed in our previous publication (Yoon S. M. et al., 2010d). Two remaining issues mentioned above are closely related to each other, because the long-time programming is definitely preferable to obtain the longer retention time. This is a kind of a severe trade-off. We have recently confirmed that the establishment of dual-gate configuration can be one of the most promising solutions to improve both requirements of the programming speed and data retention (Yoon S. M. et al., 2011b). Although the polymeric ferroelectric material was fixed in this work, it can be also possible to enhance overall performances of device by employing a new ferroelectric material. We sure that the programming and memory behaviors of the fabricated plastic memory TFT will be much improved by developing the suitable methodologies from now on.

6. Conclusion

In this work, we proposed and demonstrated the plastic nonvolatile memory TFT employing the ferroelectric copolymer gate insulator and oxide semiconductor active channel as a memory component for the flexible-type electronic devices. The device structure was designed to be Au/150 nm P(VDF-TrFE)/6 nm Al_2O_3/10 nm ZnO/Ti/Au/Ti/PEN. Firstly, the sound ferroelectric characteristics of the fabricated flexible P(VDF-TrFE) capacitors were well confirmed, that was of important in that they could be obtained with fully lithography-compatible process even on the PEN substrate at the temperature as low as 150 °C. The basic properties such as P_r, E_c, and polarization saturation behaviors with the increase in E were observed to not be so markedly varied with the changes in the R under the substrate bending situations. Then, the memory characteristics of the fabricated plastic memory TFTs with W/L of 40/20 μm were also evaluated, in which a 3.4 V memory window and 8-orders-of magnitude on/off ratio were successfully obtained. These characteristics did not experience so marked degradations at the bending situation with R of 0.97 cm and after the repetitive bending of 20000 cycles. We can conclude from the obtained results that our proposed hybrid plastic memory TFT can be a suitable candidate for an embeddable memory device

to realize the low-cost flexible electronic applications. However, as future works, the bending characteristics of the device will be more systematically investigated when the devices are bent with smaller *R*, which provides useful insights to design the flexible memory TFTs with excellent performances. The enhancements in programming and retention behaviors are also demanding for various flexible applications.

7. References

Aizawa, K. et al. (2004). Impact of HfO_2 buffer layers on data retention characteristics of ferroelectric-gate filed-effect transistors. *Applied Physics Letters*, Vol. 85, 3199-3201.

Baeg, K. J. et al. (2010). Controllable Shifts in Threshold Voltage of Top-Gate Polymer Field-Effect Transistors for Applications in Organic Nano Floating Gate Memory. *Advanced Functional Materials*, Vol. 20, 224-230.

Cho, B. et al. (2010) Electrical characterization of organic resistive memory with interfacial oxide layers formed by O_2 plasma treatment. *Applied Physics Letters*, Vol. 97, 063305.

Choi, C. W. et al. (2008). Comparative electrical bistable characteristics of ferroelectric poly(vinylidene fluoride-trifluoroethylene) copolymer based nonvolatile memory device architectures. *Applied Physics Letters*, Vol. 93, 182902.

Chu, L. W. et al. (2010). Design of Analog Pixel Memory Circuit with Low Temperature Polycrystalline Silicon TFTs for Low Power Application. *Symposium on Information Display Tech. Dig.* pp.1363-1366.

Forrest, S. R. (2004). The path to ubiquitous and low-cost organic electronic appliances on plastic. *Nature*, Vol. 428, 911-918.

Furukawa, T. (1989). Ferroelectric properties of vinylidene fluoride copolymers. *Phase Transition*, Vol. 18, 143-211.

Furukawa, T.; Nakajima, T. & Takahashi, Y. (2006). Factors Governing Ferroelectric Switching Characteristics of Thin VDF/TrFE Copolymer Films. *IEEE Transactions on Dielectrics and Electrical Insulation*, Vol. 13, 1120-1131.

Furukawa, T. et al. (2009). Ferroelectric switching dynamics in VDF-TrFE copolymer thin films spin coated on Si substrate. *Journal of Applied Physics*, Vol. 105, 061636.

Gelinck, G. H. & Leeuw, D. M. (2004). Flexible active-matirx displays and shift registers based on solution-processed organic transistors. *Nature Materials*, Vol. 3, 106-110.

Graz, I. M. & Lacour, S. P. (2009). Flexible pentacene organic thin film transistor circuits fabricated directly onto elastic silicone membranes. *Applied Physics Letters*, Vol. 95, 243305.

Horiuchi, T. et al. (2010). Lowered operation voltage in $Pt/SBi_2Ta_2O_9/HfO_2/Si$ ferroelectric-gate field-effect transistors by oxynitriding Si. *Semiconductor Science and Technology*, Vol. 25, 055005.

Hoshino, K. et al. (2009) Constant-Voltage-Bias Stress Testing of a-IGZO Thin-Film Transistors. *IEEE Transaction Electron Devices*, Vol. 56, 1365-1370.

Ishida, K. et al. (2010). User Customizable Logic Paper (UCLP) with Organic Sea-of-Transmission-Gates (SOTG) Architecture and Ink-Jet Printed Interconnects. *IEEE International Solid-State Circuits Conference Tech. Dig.*, pp. 138-139.

Ito, D. et al. (2003). Ferroelectric properties of $YMnO_3$ epitaxial films for ferroelecric-gate field-effect transistors. *Journal of Applied Physics*, Vol. 93, 5563-5567.

Jeong, J. K. et al. (2008). Origin of threshold voltage instability in indium-gallium-zinc oxide thin film transistors. *Applied Physics Letters*, Vol. 93, 123508.

Ji, Y. et al. (2010). Stable Switching Characteristics of Organic Nonvolatile Memory on a Bent Flexible Substrate. *Advanced Materials*, Vol. 22, 3071-3075.

Jung, M. et al. (2010). All-Printed and Roll-to-Roll-Printable 13.56-MHz-Operated 1-bit RF Tag on Plastic Foils. *IEEE Transaction Electron Devices*, Vol. 57, 571-580.

Kang, S. J. et al. (2008). Spin cast ferroelectric beta poly(vinylidene fluoride) thin films via rapid thermal annealing. *Applied Physics Letters*, Vol. 92, 012921.

Kang, S. J. et al. (2009). Non-volatile Ferroelectric Poly(vinylidene fluoride-co-trifluoroethylene) Memory Based on a Single-Crystalline Tri-isopropylsilylethynyl Pentacene Field-Effect Transistor. *Advanced Functional Materials*, Vol. 19, 1609-1616.

Kang, S. J. et al. (2009). Printable Ferroelectric PVDF/PMMA Blend Films with Ultralow Roughness for Low Voltage Non-Volatile Polymer Memory. *Advanced Functional Materials*, Vol. 19, 2812-2819.

Kim, K. H. (1998). Metal-ferroelectric-semiconductor (MFS) FET's using $LiNbO_3$/Si(100) structures for nonvolatile memory applications. *IEEE Electron Device Letters*, Vol. 19, 204-206.

Lee, K. H. et al. (2009). High-Mobility Nonvolatile Memory Thin-Film Transistors with a Ferroelectric Polymer Interfacing ZnO and Pentacene Channels. *Advanced Materials*, Vol. 21, 4287-4291.

Lee, K. H. et al. (2009). Flexible low voltage nonvolatile memory transistors with pentacene channel and ferroelectric polymer. *Applied Physics Letters*, Vol. 94, 093304.

Lee, M. J. et al. (2009). Low-Temperature-Grown Transition Metal Oxide Based Storage Materials and Oxide Transistors for High-Density Non-volatile Memory. *Advanced Functional Materials*, Vol. 19, 1587-1593.

Lee, N. Y. et al. (2003). Material design schemes for single-transistor-type ferroelectric memory cells using Pt/$(Bi,La)_4Ti_3O_{12}$/ONO/Si structures. *Japanese Journal of Applied Physics*, Vol. 42, 6955-6959.

Lee, S. et al. (2009). Resistive switching characteristics of ZnO thin film grown on stainless steel for flexible nonvolatile memory devices. *Applied Physics Letters*, Vol. 95, 262113.

Leong, W. L. et al. (2008). Non-Volatile Organic Memory Applications Enabled by In Situ Synthesis of Gold Nanoparticles in a Self-Assembled Block Copolymer. *Advanced Materials*, Vol. 20, 2325-2331.

Li, J. et al. (2010). A low-temperature crystallization path for device-quality ferroelectric films. *Applied Physics Letters*, Vol. 97, 102905.

Li, T. et al. (2003). The thermal stability of one-transistor ferroelectric memory with Pt-$Pb_5Ge_3O_{11}$-Ir-Poly-SiO_2-Si gate stack, *IEEE Electron Device Letters*, Vol. 50, 2280-2282.

Lim, S. H.; Rastogi, A. C. & Desu, S. B. (2004). Electrical properties of metal-ferroelectric-insulator-semiconductor structures based on ferroelectric polyvinylidene fluoride copolymer film gate for nonvolatile random access memory application. *Journal of Applied Physics*, Vol. 96, 5673-5682.

Lin, C. M.; Shih, W. C. & Lee, J. Y. (2009). Electrical characteristics of metal-ferroelectric ($BiFeO_3$)-insulator (Y_2O_3)-semiconductor capacitors and field-effect transistors. *Applied Physics Letters*, Vol. 94, 142905.

Lin, K. L. & Jain, K. (2009). Design and Fabrication of Stretchable Multilayer Self-Aligned Interconnects for Flexible Electronics and Large-Area Sensor Arrays Using Excimer Laser Photoablation. *IEEE Electron Device Letters*, Vol. 30, 14-16.

Ma, L. et al. (2002). Organic electrical bistable devices and rewritable memory cells. *Applied Physics Letters*, Vol. 80, 2997-2999.

Ma, L.; Xu, Q. & Yang, Y. (2004). Organic nonvolatile memory by controlling the dynamic copper-ion concentration within organic layer. *Applied Physics Letters*, Vol. 84, 4908-4910.

Matsumoto, A. et al. (2007). Ferro- and piezoelectric properties of vinylidene fluoride oligomer thin film fabricated on flexible polymer film. *Applied Physics Letters*, Vol. 90, 202906.

Nalwa, H. S. (1995) *Ferroelectric Polymers: Chemistry, Physics and Applications*, Marcel Dekker.

Naber, R. C. G. et al. (2005). High-performance solution-processed polymer ferroelectric field-effect transistors. *Nature Materials*, Vol. 4, 243-248.

Naber, R. C. G. et al. (2005). An Organic Field-Effect Transistor with Programmable Polarity. *Advanced Materials*, Vol. 17, 2692-2695.

Nguyen, C. A. et al. (2008). Enhanced organic ferroelectric field effect transistor characteristics with strained poly(vinylidene fluoride-trifluoroethylene) dielectric. *Organic Electronics*, Vol. 9, 1087-1092.

Noh, S. H. et al. (2007) ZnO-based nonvolatile memory thin-film transistors with polymer dielectric/ferroelectric double gate insulators. *Applied Physics Letters*, Vol. 90, 253504.

Nomura, K. et al. (2004). Room-temperature fabrication of transparent flexible thin-film transistors using amorphous oxide semiconductors. *Nature*, Vol. 432, 488-492.

Novak, M. et al. (2010). Flexible copper-7,7,8,8 tetracyanochinodimethane memory devices-Operation, cross talk and bending. *Thin Solid Films*, Vol. 518, 2222-2227.

Osada, T. et al. (2010). Development of Liquid Crystal Display Panel Integrated with Drivers Using Amorphous In-Ga-Zn-Oxide Thin Film Transistors. *Japanese Journal of Applied Physics*, Vol. 49, 03CC02.

Ohara, H. et al. (2010). 4.0-inch Active-Matrix Organic Light-Emitting Diode Display Integrated with Driver Circuits Using Amorphous In-Ga-Zn-Oxide Thin-Film Transistors with Suppressed Variation, *Japanese Journal of Applied Physics*, Vol. 49, 03CD02.

Park, C. H. et al. (2009) Enhancing the retention properties of ZnO memory transistor by modifying the channel/ferroelectric polymer interface. *Applied Physics Letters*, Vol. 95, 153502.

Park, J. S. et al. (2009). Flexible full color organic light-emitting diode display on polyimide plastic substrate driven by amorphous indium gallium zinc oxide thin-film transistors. *Applied Physics Letters*, Vol. 95, 013503.

Park, S. H. et al. (2009). Transparent and Photo-stable ZnO Thin-film Transistors to Drive an Active Matrix Organic-Light-Emitting-Diode Display Panel. *Advanced Materials*, Vol.21, 678-682.

Roh, J. et al. (2010) $PbZr_xTi_{1-x}O_3$ Ferroelectric Thin-Film Capacitors for Flexible Nonvolatile Memory Applications. *IEEE Electron Device Letters*, Vol. 31, 1017-1019.

Sekitani, T. et al. (2009). Stretchable active-matrix organic light-emitting diode display using printable elastic conductors. *Nature Materials*, Vol. 8, 494-499.

Sekitani, T. et al. (2009). Printed Nonvolatile Memory for a Sheet-Type Communication System. *IEEE Transaction Electron Devices*, Vol. 56, 1027-1035.

Seo, J. W. et al. (2009). Transparent flexible resistive random access memory fabricated at room temperature. *Applied Physics Letters*, Vol. 95, 133508.

Shih, W. C.; Kang, K. & Lee, J. Y. (2007). The improvement of retention time of metal-ferroelectric ($PbZr_{0.53}Ti_{0.47}O_3$)-insulator (Y_2O_3)-semiconductor transistors by surface treatments. *Applied Physics Letters*, Vol. 91, 232908.

Schroeder, R.; Majewski, L. A. & Grell, M. (2004). All-organic permanent memory transistor using an amorphous, spin-cast ferroelectric-like gate insulator. *Advanced Materials*, Vol. 16, 633-636.

Someya, T. et al. (2005). Integration of organic FETs with organic photodiodes for a large area, flexible, and lightweight sheet image scanners. *IEEE Transaction Electron Devices*, Vol. 52, 2502-2511.

Tokumitsu, E.; Nakamura, R. & Ishiwara, H. (1997). Nonvolatile Memory Operations of Metal-Ferroelectric-Insulator-Semiconductor (MFIS) FET's Using PLZT/STO/Si(100) Structures. *IEEE Electron Device Letters*, Vol. 18, 160-162.

Tokumitsu, E.; Fujii, G. & Ishiwara, H. (1999). Nonvolatile ferroelectric-gate field-effect transistors using $SrBi_2Ta_2O_9$/Pt/$SrTa_2O_6$/SiON/Si structures. *Applied Physics Letters*, Vol. 75, 575-577.

Ueda, N. et al., (2010). A Novel Multi-level Memory in Pixel Technology for Ultra Low Power LTPS TFT-LCD. *Symposium on Information Display Tech. Dig.* pp.615-618.

Uni, K. N. N. et al. (2004). A nonvolatile memory element based on an organic field-effect transistor. *Applied Physics Letters*, Vol. 85, 1823-1825.

Wang, W.; Shi, J. & Ma, D. (2009). Organic Thin-Film Transistor Memory With Nanoparticle Floating Gate. *IEEE Transaction Electron Devices*, vol. 56, 1036-1039.

Yoon, S. M.; Tokumitsu, E. & Ishiwara, H. (1999). Adaptive-learning neuron integrated circuits using metal-ferroelectric ($SrBi_2Ta_2O_9$)-semiconductor (MFS) FET's. *IEEE Electron Device Letters*, Vol. 20, 526-528.

Yoon, S. M. et al. (2009). Effect of ZnO channel thickness on the device behaviour of nonvolatile memory thin film transistors with double-layered gate insulators of Al_2O_3 and ferroelectric polymer. *Journal of Physics D*, Vol. 42, 245101.

Yoon, S. M. et al. (2009). Effects of Chemical Treatments on the Electrical Behaviors of Ferroelectric Poly(vinylidene fluoride-trifluoroethylene) Copolymer for Nonvolatile Memory Device Applications. *Japanese Journal of Applied Physics*, Vol. 48, 09KA20.

Yoon, S. M. et al. (2010). Impact of interface controlling layer of Al_2O_3 for improving the retention behaviors of In-Ga-Zn oxide-based ferroelectric memory transistor. *Applied Physics Letters*, Vol. 96, 232903.

Yoon, S. M. et al. (2010). Fully Transparent Non-volatile Memory Thin-Film Transistors Using an Organic Ferroelectric and Oxide Semiconductor Below 200 °C. *Advanced Functional Materials*, Vol. 20, 921-926.

Yoon, S. M. et al. (2010). Nondestructive Readout Operation of Oxide-Thin-Film-Transistor-Based 2T-Type Nonvolatile Memory Cell. *IEEE Electron Device Letters*, Vol. 31, 138-140.

Yoon, S. M. et al. (2010). Characterization of Nonvolatile Memory Behaviors of Al/Poly(vinylidene fluoride.trifluoroethylene)/Al_2O_3/ZnO Thin-Film Transistors. *Japanese Journal of Applied Physics*, Vol. 49, 04DJ06.

Yoon, S. M. et al. (2011). Nonvolatile Memory Thin-Film Transistors using Organic Ferroelectric Gate Insulator and Oxide Semiconducting Channel. *Semiconductor Science and Technology*, Vol. 26, 034007.

Yoon, S. M. et al. (2011). Oxide Semiconductor-Based organic/Inorganic Hybrid Dual-Gate Nonvolatile Memory Thin-film Transistor. *IEEE Transaction Electron Devices* (To be published)

Zschieschang, U. et al., (2010). Flexible Low-Voltage Organic Transistors and Circuits Based on a High-Mobility Organic Semiconductor with Good Air Stability. *Advanced Materials*, Vol. 22, 982-985.

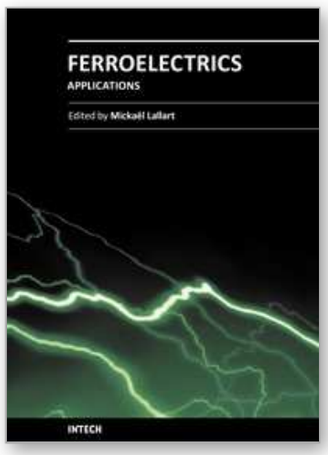

Ferroelectrics - Applications

Edited by Dr. MickaÃ«l Lallart

ISBN 978-953-307-456-6
Hard cover, 250 pages
Publisher InTech
Published online 23, August, 2011
Published in print edition August, 2011

Ferroelectric materials have been and still are widely used in many applications, that have moved from sonar towards breakthrough technologies such as memories or optical devices. This book is a part of a four volume collection (covering material aspects, physical effects, characterization and modeling, and applications) and focuses on the application of ferroelectric devices to innovative systems. In particular, the use of these materials as varying capacitors, gyroscope, acoustics sensors and actuators, microgenerators and memory devices will be exposed, providing an up-to-date review of recent scientific findings and recent advances in the field of ferroelectric devices.

How to reference

In order to correctly reference this scholarly work, feel free to copy and paste the following:

Sung-Min Yoon, Shinhyuk Yang, Soon-Won Jung, Sang-Hee Ko Park, Chun-Won Byun, Min-Ki Ryu, Himchan Oh, Chi-Sun Hwang, Kyoung-Ik Cho and Byoung-Gon Yu (2011). Ferroelectric Copolymer-Based Plastic Memory Transistors, Ferroelectrics - Applications, Dr. MickaÃ«l Lallart (Ed.), ISBN: 978-953-307-456-6, InTech, Available from: http://www.intechopen.com/books/ferroelectrics-applications/ferroelectric-copolymer-based-plastic-memory-transistors

INTECH
open science | open minds

InTech Europe
University Campus STeP Ri
Slavka Krautzeka 83/A
51000 Rijeka, Croatia
Phone: +385 (51) 770 447
Fax: +385 (51) 686 166
www.intechopen.com

InTech China
Unit 405, Office Block, Hotel Equatorial Shanghai
No.65, Yan An Road (West), Shanghai, 200040, China
中国上海市延安西路65号上海国际贵都大饭店办公楼405单元
Phone: +86-21-62489820
Fax: +86-21-62489821

IntechOpen